Published in final edited form as:
J Mater Sci Mater Med. 2013 November ; 24(11): . doi:10.1007/s10856-013-5006-2.

Carbonic anhydrase immobilized on hollow fiber membranes using glutaraldehyde activated chitosan for artificial lung applications

J. D. Kimmel,
McGowan Institute for Regenerative Medicine, University of Pittsburgh, 3025 East Carson Street, Pittsburgh, PA 15203, USA. Department of Bioengineering, University of Pittsburgh, Pittsburgh, PA, USA

D. T. Arazawa,
McGowan Institute for Regenerative Medicine, University of Pittsburgh, 3025 East Carson Street, Pittsburgh, PA 15203, USA. Department of Bioengineering, University of Pittsburgh, Pittsburgh, PA, USA

S.-H. Ye,
McGowan Institute for Regenerative Medicine, University of Pittsburgh, 3025 East Carson Street, Pittsburgh, PA 15203, USA. Department of Surgery, University of Pittsburgh Medical Center, Pittsburgh, PA, USA

V. Shankarraman,
McGowan Institute for Regenerative Medicine, University of Pittsburgh, 3025 East Carson Street, Pittsburgh, PA 15203, USA. Department of Surgery, University of Pittsburgh Medical Center, Pittsburgh, PA, USA

W. R. Wagner, and
McGowan Institute for Regenerative Medicine, University of Pittsburgh, 3025 East Carson Street, Pittsburgh, PA 15203, USA. Department of Bioengineering, University of Pittsburgh, Pittsburgh, PA, USA. Department of Surgery, University of Pittsburgh Medical Center, Pittsburgh, PA, USA. Department of Chemical and Petroleum Engineering, University of Pittsburgh, Pittsburgh, PA, USA

W. J. Federspiel
McGowan Institute for Regenerative Medicine, University of Pittsburgh, 3025 East Carson Street, Pittsburgh, PA 15203, USA. Department of Bioengineering, University of Pittsburgh, Pittsburgh, PA, USA. Department of Chemical and Petroleum Engineering, University of Pittsburgh, Pittsburgh, PA, USA. Department of Critical Care Medicine, University of Pittsburgh Medical Center, Pittsburgh, PA, USA

W. J. Federspiel: federspielwj@upmc.edu

Abstract

Extracorporeal CO_2 removal from circulating blood is a promising therapeutic modality for the treatment of acute respiratory failure. The enzyme carbonic anhydrase accelerates CO_2 removal within gas exchange devices by locally catalyzing HCO_3^- into gaseous CO_2 within the blood. In this work, we covalently immobilized carbonic anhydrase on the surface of polypropylene hollow

Correspondence to: W. J. Federspiel, federspielwj@upmc.edu.

Disclosures W. J. Federspiel is a co-founder and shareholder in ALung Technologies.

fiber membranes using glutaraldehyde activated chitosan tethering to amplify the density of reactive amine functional groups for enzyme immobilization. XPS and a colorimetric amine assay confirmed higher amine densities on the chitosan coated fiber compared to control fiber. Chitosan/CA coated fibers exhibited accelerated CO_2 removal in scaled-down gas exchange devices in buffer and blood (115 % enhancement vs. control, 37 % enhancement vs. control, respectively). Carbonic anhydrase immobilized directly on hollow fiber membranes without chitosan tethering resulted in no enhancement in CO_2 removal. Additionally, fibers coated with chitosan/carbonic anhydrase demonstrated reduced platelet adhesion when exposed to blood compared to control and heparin coated fibers.

1 Introduction

Extracorporeal respiratory assist devices perform O_2 and CO_2 exchange independent of lung tissues, allowing the lungs to rest and recover during acute respiratory failure. Use of such devices has been proposed as a viable alternative or adjuvant therapy to invasive mechanical ventilation (MV) [1, 2], which has serious complications including mechanical lung trauma, systemic inflammatory mediator release and infection [3, 4], leading to increased mortality and morbidity rates [5, 6]. Sufficient CO_2 removal from the blood, rather than O_2 delivery, is often a primary obstacle for the treatment of acute respiratory failure [7, 8]. New devices specifically focused on extracorporeal CO_2 removal ($ECCO_2R$) are designed to remove CO_2 at low blood flow rates [9–11], which permits minimally invasive vascular access and reduced trauma to the blood. Novel coatings on gas exchange membranes which accelerate CO_2 removal while providing sufficient hemocompatibility may lead to the next generation of highly efficient $ECCO_2R$ devices for the treatment of severe respiratory failure.

Most of the CO_2 carried in the blood (>90 %) is in the form of bicarbonate (HCO_3^-), which is reversibly catalyzed to gaseous CO_2 within red blood cells by the enzyme carbonic anhydrase (CA):

$$CO_2 + H_2O \overset{CA}{\Longleftrightarrow} HCO_3^- + H^+$$

$ECCO_2R$ gas exchange membranes cannot remove bicarbonate from the blood, hence, CO_2 removal rates within $ECCO_2R$ devices are limited by endogenous $HCO_3^- \rightarrow CO_2$ catalysis. We previously demonstrated enhanced CO_2 removal by covalently immobilizing CA directly on the surface of hollow fiber membranes (HFMs), which locally converts bicarbonate to gaseous CO_2 at the fiber surface, resulting in increased blood-side CO_2 partial pressure and accelerated CO_2 flux through the membrane [12, 13]. In this work, we developed a new coating technology using glutaraldehyde activated chitosan to covalently tether CA to the surface of HFMs used in a commercial $ECCO_2R$ device (Hemolung, ALung Technologies). We hypothesized that an amine (NH_2) rich polymer such as chitosan would serve as an ideal support for covalent immobilization of CA to the polypropylene HFM surface using amine-reactive glutaraldehyde chemistry. We also investigated platelet adsorption using fibers coated with chitosan and CA compared to heparin coated fibers currently used in the commercial Hemolung device. The Hemolung has demonstrated efficacy in reducing blood pCO_2 levels and MV dependence in hypercapnic animal models [14, 15], and was successful in preventing the need for MV in humans with chronic obstructive pulmonary disease (COPD) in a pilot clinical trial. However, further enhancement in CO_2 removal rates and device hemocompatibility using CA immobilized HFMs offers significant potential to improve patient outcomes in the setting of severe respiratory failure.

Proper functionality of the CA coating depends on sufficient loading of CA molecules on the fiber surface, and maintained catalytic activity of the immobilized CA. Improvement in immobilized enzyme activity through use of a tethering molecule such as polyethylene glycol (PEG) is well established [16–18]. Reduced steric hindrance between neighboring enzyme molecules and improved presentation of the enzymatic active site are putative results from attachment to a polymeric tethering agent, compared to direct enzyme immobilization on the surface [19]. Additionally, branched or multifunctional polymer molecules possess the ability to amplify the density of reactive functional groups available for covalent attachment of the desired biomolecule [20, 21]. In this application, we hypothesized that increased amine group densities using chitosan tethering would lead to increased levels of bound CA on the HFMs, and higher levels of CO_2 removal in a scaled-down gas exchange device. Lastly, immobilization of hydrophilic polymeric molecules on blood contacting surfaces has been shown to prevent protein adsorption and subsequent platelet activation, which are significant goals in the development of next generation medical device coatings.

Chitosan is a natural polysaccharide formed from deacetylation of chitin, comprised of varying ratios of D-glucosamine and *N*-acetyl residues. Chitosan has garnered a great deal of interest in recent years for use in biomedical applications due to its excellent biocompatibility and biodegradability, low toxicity, anti-bacterial properties, and abundant supply from natural sources [22]. Chitosan has been used as a tethering agent for enzyme immobilization for a variety of applications, including immunoassays [23], bioremediation [24], and industrial biocatalysis [25]. However, in these applications gas permeability of the chitosan layer is not an important objective, whereas maintaining sufficient gas exchange through the coated fiber membrane is critical in respiratory assist devices. The goal of this work was to develop a high efficiency CA coating using glutaraldehyde activated chitosan tethering, capable of improving CO_2 removal while mitigating deleterious effects on fiber gas permeance. The proposed glutaraldehyde coating technology is straightforward, low cost, and free of harsh organic solvents. Lastly, we sought to characterize platelet adsorption properties of the chitosan/CA coated fiber compared to traditional heparin coated fibers used in a clinical device.

2 Materials and methods

2.1 Materials

Commercial microporous polypropylene HFMs (Celgard™; Membrana GmbH, Wuppertal, Germany) were coated with a thin siloxane layer and functionalized with amine groups using proprietary plasma enhanced chemical vapor deposition (PECVD) processes by ALung Technologies (Pittsburgh, PA). Chitosan (MW = 50–190 kD, based on viscosity), glutaraldehyde, dimethylformamide, Triton X-100, perchloric acid and glacial acetic acid were purchased from Sigma Aldrich (St. Louis, MO). Sulfosuccin-imidyl-4-0-(4,4′-dimethoxytrityl) butyrate (sulfo-SDTB) was purchased from Prochem, Inc. (Rockford, IL). All other reagents were of analytical grade or greater. Recombinant human CA II was provided by Dr. D. Silverman and Dr. R. McKenna at the University of Florida. CA II was purified from transfected *Escherichia coli* lysate using affinity chromatography, dialysis and ultrafiltration, as reported previously [26]. Purity was characterized using gel electrophoresis and was determined to be >95 %.

2.2 Carbonic anhydrase immobilization

CA was covalently linked to the HFM surface via glutaraldehyde crosslinking, with and without the use of chitosan tethering. Preliminary work evaluating other amine rich polymers such as polyethylene imine (PEI) and poly-L lysine (PLL) demonstrated poor

performance compared to chitosan. As such, chitosan was chosen as the ideal candidate for the purposes of this study. Aminated knitted HFM mats (204 cm^2 fiber surface area) were incubated in 5 % glutaraldehyde in 100 mM phosphate buffer (PB), pH 8.5 for 1 h under constant rocking at ambient temperature. Fibers were then rinsed with deionized (DI) water, and washed three times with PB for 10 min each wash cycle. Chitosan was linked to the fiber via covalent binding between amine groups on the chitosan polymer and glutaraldehyde-activated amine groups on the HFM. Chitosan powder was dissolved in 1 % acetic acid (1:99 acetic acid:DI water) to obtain a 1 % chitosan solution (w/v). Fibers were incubated in the chitosan solution for 1 h under constant rocking at ambient temperature. Fibers were then rinsed with PB as previously described. A second glutaraldehyde incubation was performed in the same manner as described above, to activate free amine groups on the chitosan polymer. After washing with PB, a CA solution (1 mg/mL in 100 mM PB, pH 8.5) was incubated with the fibers to covalently link glutaraldehyde-activated amine groups on the chitosan polymer to surface amine groups on the CA molecule. Fibers were incubated with the CA solution for 15 h under constant rocking at ambient temperature. Unbound CA was removed from the fiber surface with triplicate washing using 100 mM PB for 15 min each cycle.

2.3 Quantification of fiber surface amine groups

Amine functional group density for control (siloxane/aminated) and chitosan immobilized fibers was quantified using a colorimetric assay as described by Cook et al. [27]. Briefly, sulfo-SDTB binds surface amine groups on the fiber, followed by perchloric acid cleavage of the sulfo-SDTB colorimetric moiety, which is quantified in the supernatant using UV–Vis spectrophotometry. Sulfo-SDTB (25 mg) was dissolved in 2 mL of dimethylformamide, and diluted into 32 mL of 0.1 M sodium carbonate buffer, pH 8.5. Fiber samples (44.5 cm^2 surface area) were incubated with 8 mL sulfo-SDTB solution for 15 min in glass tubes, while continuously rocked at ambient temperature. Samples were rinsed consecutively with 1 M NaCl, 0.5 % Tween-20 in DI water, and pure DI water, each for 20 min to remove unbound sulfo-SDTB. Fiber samples were placed in new glass tubes and incubated with 35 % perchloric acid for 10 min until the fluid developed an orange color. Aliquots were removed and quantified for absorbance at 498 nm using a UV–Vis spectrophotometer (Thermo Fisher Scientific, Waltham, MA). A standard curve was generated by serially diluting known concentrations of sulfo-SDTB solution in 35 % perchloric acid. Fiber surface amine density (nmol/cm^2) was calculated by interpolating sample absorbance values with the standard curve, assuming 1:1 binding of sulfo-SDTB to surface amine groups, and a single colorimetric moiety per sulfo-SDTB molecule.

2.4 XPS analysis of fiber samples

Fiber samples were characterized using XPS to analyze surface chemistry changes from chitosan immobilization. Control and chitosan modified fibers were analyzed using a Surface Science Instruments S-probe spectrometer at the University of Washington National ESCA and Surface Analysis Center for Biomedical Problems (Seattle, WA). Three 800 μm spots were analyzed for each sample, using 150 eV pass energy and take off angle of 55°. Service Physics ESCA2000A Analysis Software was used to determine peak areas and to calculate elemental compositions from peak areas above a linear background.

2.5 Fiber gas permeance

CO_2 gas permeance of fiber samples was tested in a gas–gas permeance setup, as previously described by Eash et al. [28]. Individual fibers were removed from knitted mats after immobilization with chitosan or chitosan+CA. One end of the fiber lumen was sealed with glue, and the other end was open to the gas outlet pathway. Single fibers were placed in nylon tubes, which were sealed at one end, causing the gas to permeate through the fiber.

The length of each fiber was measured to calculate surface area of exposed fiber, which was used to normalize gas permeance measurements. CO_2 gas was introduced to the sealed fiber segments at a constant pressure of 500 mmHg at ambient temperature, and outlet CO_2 gas flow was measured using a bubble flow meter. Three fiber samples were measured for each immobilization condition, with three flow measurements recorded for each sample. Gas permeance was calculated using $K = Q/(A * \Delta P)$ where K is gas permeance, Q is measured gas flow rate, A is fiber surface area, and ΔP is the differential pressure across the fiber.

2.6 In vitro CO_2 removal

HFM bundles were potted into scaled-down gas exchange modules (0.0119 m^2) to characterize CO_2 removal efficacy. Module potting and the in vitro gas exchange apparatus was described by our group previously [12]. The fluid flow loop consisted of the scaled-down gas exchange module connected in series with a peristaltic pump, Minimax Plus pediatric oxygenator (Medtronic, Minneapolis, MN), heat exchanger, and closed liquid reservoir. The oxygenator was used to maintain a constant CO_2 partial pressure (pCO_2) of ~50 mmHg at the test module inlet. The gas flow loop consisted of the gas exchange module connected in series with pure oxygen sweep gas maintained by a mass flow controller (Fathom Technologies, Georgetown, TX), liquid condenser, vacuum pump, and an inline infrared CO_2 analyzer (PP Systems, Amesbury, MA). A schematic of the gas exchange test loop is shown in Fig. 1.

Gas exchange experiments were performed in phosphate buffered saline (PBS) and bovine blood. For the PBS experiments, NaOH was initially titrated into 10 mM PBS to ~pH 12, such that when CO_2 was introduced to the test loop fluid, the PBS pH equilibrated to physiologic values (7.3–7.4) due to $CO_2 \rightarrow HCO_3^- \rightarrow H^+$ acidification. Heparinized bovine blood was purchased from Lampire Biological Labs (Pipersville, PA), and glucose was adjusted to 100–300 mg/dL prior to use by the addition of 5 % dextrose solution. CO_2 partial pressure in the fluid was quantified at the inlet of the test module using a RapidLab 248 blood gas analyzer (Siemens, Deerfield, IL). For all experiments, the system was maintained at 37 °C, 50 mmHg pCO_2, and 45 mL/min liquid flow rate unless stated otherwise. Oxygen sweep gas flow rate was maintained to minimize buildup of CO_2 in the fiber lumen, which adversely affects the transmembrane CO_2 partial pressure gradient driving force [29]. Gas flow rate was set for each test module at a value which maintained a CO_2 concentration of ~3,000 ppm in the outflow. Preliminary experiments determined that this low level of CO_2 in the sweep gas did not impact gas exchange performance (data not shown). In this manner, we compared gas exchange modules with different CO_2 removal efficiencies by maintaining a constant CO_2 concentration in the sweep gas stream, and varied the sweep gas flow rate to determine overall CO_2 removal rates.

2.7 Imaging and quantification of adhered platelets

Whole ovine blood was collected via jugular venipuncture with an 18-gauge 1.5-in. needle into a syringe containing heparin (6.0 U/mL) after discarding the first 3 mL. Institutional Animal Care and Use Committee (IACUC) guidelines for the care and use of laboratory animals were observed. HFM samples (control, chitosan immobilized, chitosan+CA immobilized, commercial heparin bonded Hemolung) were cut into 10 cm segments (0.94 cm^2 surface area) and fiber ends were sealed with glue. Fiber samples were then sterilized with 70 % ethanol and rinsed with 0.9 % NaCl. Fiber samples were placed into BD Vacutainer blood collection tubes (BD Biosciences, Franklin Lakes, NJ) and filled with 5 mL of heparinized ovine blood. After continuous rocking for 2 h at 37 °C on a hematology mixer (Fisher Scientific, Pittsburgh, PA), HFM samples were rinsed thoroughly with PBS and immersed in a 2.5 % glutaraldehyde solution for 2 h at 4 °C to fix the surface adherent platelets. Adhered platelets were then serially dehydrated with a series of ethanol/water

mixtures (30, 50, 70, 90, 100 % (v/v)) and dried after immersion in hexamethylene disilazane for 15 min. Each fiber sample was observed by scanning electron microscopy (JSM-6330F, JEOL USA, Inc., Peabody, MA) after the surfaces were sputter coated with gold/palladium.

For adherent platelet quantification, fiber samples were collected after blood exposure as described above, rinsed thoroughly with PBS, and immersed in 0.5 mL of 2 % Triton X-100 solution for 20 min to lyse surface adhered platelets. Deposited platelets on each surface were quantified by a lactate dehydrogenase (LDH) assay [30] with an LDH Cytotoxicity Detection Kit (Clontech Laboratories, Inc. Mountain View, CA). Calibration of spectrophotometer absorbance results to platelet numbers was accomplished using a calibration curve generated from known dilutions of ovine platelet rich plasma in the lysing solution.

2.8 Statistical analysis

LDH assay results are presented as means (number of adherent platelets/cm^2) with standard deviation ($n = 3$ separate blood draws for each fiber sample). Statistical significance between sample groups was determined using ANOVA followed by post hoc Newman–Keuls testing of specific differences. All other data was compared using a Student's t test, statistical significance was considered to exist at $p < 0.05$.

3 Results

3.1 Quantification of fiber surface amine groups

Reactive amine group density on the fiber surface was compared for control (siloxane/aminated) and chitosan immobilized fibers using a colorimetric sulfo-SDTB amine assay ($n = 4$ for each group). Results illustrated in Fig. 2 indicate that fibers modified with chitosan had substantially higher amine densities than control fibers (3.3 vs. 0.67 nmol/cm^2, respectively, $p < 0.05$).

3.2 XPS and SEM analysis

Chemical surface analysis of control and chitosan fiber samples was utilized to characterize surface modification from chitosan immobilization, and provide secondary confirmation of results from the colorimetric amine assay which indicated higher amine density for the chitosan immobilized fibers compared to control fibers. XPS atomic surface composition for control and chitosan immobilized fibers is illustrated in Table 1. Control fibers contain predominantly carbon, oxygen and silicon, consistent with a siloxane coating applied by the manufacturer, and a small amount of nitrogen from the PECVD amine grafting. The chitosan immobilized fibers contain significantly less silicon, due to coverage of the underlying siloxane coating. Additionally, the chitosan fibers contain more than double the nitrogen content compared to control fibers, which can be interpreted as amine groups, since no other source of nitrogen exists in the chitosan polymer. Overall, XPS results indicate immobilization of chitosan on the HFM surface, and amplification of surface amine groups compared to control fibers.

SEM images illustrated in Fig. 3 show the fiber surface before (control) and after chitosan/CA immobilization. In the control sample, the siloxane layer applied by the manufacture is evident, obscuring the pore structure of the membrane. After chitosan/CA immobilization, small aggregates are observed throughout the fiber surface. The coating appears to be comprised of local deposits of chitosan and CA, rather than a continuous coating evenly dispersed on the membrane.

3.3 In vitro CO_2 removal

HFM modules modified with chitosan and CA were characterized for CO_2 removal in PBS and bovine blood. HFMs modified with only chitosan, only CA, and chitosan+CA, were compared to control HFMs ($n = 2$ for each group). As illustrated in Fig. 4a, chitosan+CA devices significantly enhanced gas exchange in PBS compared to control devices (196.6 vs. 91.5 mL/min m^2, respectively), whereas devices modified with only chitosan or only CA did not increase CO_2 removal. Chitosan/CA modified HFM devices also enhanced CO_2 removal in blood compared to control fibers, as illustrated in Fig. 4b, although to a lesser extent than was observed in PBS (37 % enhancement vs. 115 % enhancement, respectively). Overall CO_2 removal rates were higher for both control and chitosan/CA modified devices in blood compared to PBS, likely due to endogenous CA in red blood cells, which helps to continually maintain blood pCO_2 through $HCO_3^- \rightarrow CO_2$ conversion.

3.4 Fiber gas permeance

CO_2 gas permeance results are shown in Fig. 5a. Chitosan and chitosan+CA fibers had the same permeance value, 8.4×10^{-4} mL/s cm^2 cmHg, less than half of the permeance observed for control fibers, 1.9×10^{-3} mL/s cm^2 cmHg. Results indicate that the chitosan coating impedes CO_2 flux through the fiber membrane in a gas–gas setup, although further studies were performed during in vitro characterization of HFM devices to examine CO_2 transport in a liquid environment, where (1) hydrogel characteristics of the chitosan polymer would be expected to alter CO_2 diffusion, and (2) inclusion of liquid boundary layer resistance would provide a more relevant description of gas transfer in the HFM device. Of note, immobilization of CA onto the chitosan coated fibers did not impact CO_2 permeance in the gas–gas experiment.

3.5 CO_2 removal versus liquid flow rate

Liquid flow rate in the device was varied to investigate mass transport characteristics of the chitosan coating, specifically, if the coating reduced CO_2 transfer compared to unmodified fibers, as was observed in the gas–gas permeance results. As expected, overall CO_2 removal rates increased with increasing flow rate for all samples tested in PBS (Fig. 5b). Chitosan and control devices had comparable CO_2 removal rates at the lowest flow rates tested (45 mL/min), but the removal curves begin to deviate with increasing flow rate, as the chitosan devices trend towards lower CO_2 removal compared to control devices. This result can be interpreted as a reduction in liquid boundary layer diffusive resistance with increasing flow rate; i.e. permeance of the fiber membrane becomes more prominent in determining gas flux as boundary layer resistance decreases. The chitosan coating reduces fiber permeance, but this effect is only relevant at high liquid flow rates, since boundary layer resistance dominates mass transport at lower flow rates.

3.6 Platelet deposition on fiber surface

Acute platelet deposition on fiber surfaces was investigated to compare hemocompatibility properties of chitosan/CA coated fibers compared to both control fibers and commercial Hemolung fibers coated with heparin. Figure 6a illustrates fiber surfaces observed by SEM after continuous ovine blood contact for 2 h at 37 °C. Maximum platelet deposition and aggregation was observed on the siloxane/aminated control fiber. Platelet deposition was reduced on Hemolung heparin coated and chitosan modified surfaces, with chitosan/CA fibers demonstrating the least amount of adhered platelets. Quantitative results from the LDH platelet assay correlated with qualitative results from the SEM images (Fig. 6b); chitosan/CA fibers exhibited the lowest levels of adsorbed platelets compared to control, Hemolung heparin, and chitosan fibers ($p < 0.05$). Some surface heterogeneity was observed

in SEM images of the chitosan and chitosan/CA coated fibers, likely due to aggregation of chitosan and/or CA during the immobilization process.

4 Discussion

The goal of this study was to develop a biocatalytic coating capable of accelerating CO_2 removal with HFMs currently used in a commercial extracorporeal respiratory assist device (Hemolung). Previous work by our group utilizing polymethylpentene fibers demonstrated enzymatically active CA coatings using radio frequency glow discharge surface modification of the fiber, followed by direct chemical attachment of CA to the fiber surface using CNBr chemistry. In this work, we developed a simple glutaraldehyde crosslinking chemistry using aminated polypropylene HFMs, and found that a polymeric chitosan tethering molecule was necessary to achieve functional attachment of the enzyme on the fibers. Use of the chitosan spacer molecule amplified surface amine groups available for CA attachment, and did not impact gas transport of the fibers under clinically relevant liquid flow rates.

Coatings for gas permeable membranes must achieve a balance between maximizing functionality of the coating while mitigating reduction in membrane gas permeance. Chitosan has been shown to be a useful tethering agent for immobilization of biomolecules to surfaces, however, this is the first study to utilize a chitosan-based bioactive coating while maintaining gas flux of the underlying membrane. Although chitosan coated fibers demonstrated reduced CO_2 permeance in a gas–gas setup, minimal effects on CO_2 removal were observed between chitosan and control gas exchange modules when tested with PBS buffer under flow conditions. Mass transport in HFM devices is dictated by diffusional resistances of the liquid boundary layer and the fiber membrane permeance. Since these resistances are in series, overall system mass transport is dominated by the largest resistance, which is typically diffusion through the liquid boundary layer [31]. In the recirculating PBS gas exchange experiment, CO_2 removal using chitosan coated fibers began to decrease with increasing liquid flow rate, compared to control fibers. Hence, as flow rate increases and boundary layer resistance decreases, the chitosan coating begins to impede CO_2 removal. However, we would not expect significant reduction in CO_2 flux under clinically relevant flow rates. In this study, liquid flow rate to surface area ratio was scaled comparable to human devices currently used for extracorporeal respiratory support. A survey of a dozen clinical device manufacturer specifications found surface area ranges from 0.6 to 2.5 m^2, and flow rate ranges from 0.35 to 7 L/min. Our scaled-down device had a surface area of 0.0119 m^2 and liquid flow rate of 45 mL/min, which is scaled appropriately to mimic the mass transport environment under clinically relevant conditions.

CA immobilization parameters utilized in this study were initially chosen based on relevant reports in the literature demonstrating suitable reagent conditions and incubation times for glutaraldehyde-crosslinked biomolecule immobilization [23, 32, 33]. However, further optimization of immobilization parameters such as reagent concentration, incubation time, and incubation temperature was performed in our laboratory to characterize effects on CA-mediated CO_2 removal. Although we did observe differences in immobilized CA activity under varied immobilization conditions, we found no significant differences in CO_2 removal rates (data not shown), likely due to dominance of blood-side liquid boundary layer resistance in dictating overall CO_2 mass transport. For the purposes of this study, we presented a representative immobilization protocol which may be further optimized for devices with different mass transport characteristics. Indeed, changes in immobilized CA concentration or activity are unlikely to result in meaningful acceleration of CO_2 removal without an accompanied decrease in boundary layer resistance.

Results from the colorimetric sulfo-SDTB amine assay and XPS surface analysis confirmed that chitosan coated fibers exhibited higher levels of surface amine groups than control fibers. Quantitative differences between the two methods in amine group ratio for chitosan coated/control fiber [2.25-fold increase (XPS) vs. 5-fold increase (sulfo-SDTB)] may be due to non-specific adsorption of the sulfo-SDTB molecule on the fiber surface. Enhanced CO_2 removal using chitosan/CA coated fibers is attributed to increased loading of CA molecules on the chitosan scaffold due to amine group amplification. Additionally, the hydrophilic properties of the chitosan polymer may have also provided an amenable microenvironment for stable CA enzymatic function, although this phenomenon needs to be investigated further.

Acute platelet deposition results indicate favorable hemocompatibility properties of the chitosan/CA fiber. Although some reports [34, 35] have suggested a tendency for chitosan to promote adherent red blood cells and platelets, we did not see evidence of this during the present study. Others have hypothesized that the cationic amine groups on the chitosan polymer may bind red blood cells [36]. Given that the CA molecule is covalently attached to free chitosan amine groups, this may help explain the dearth of red cell and platelet adhesion in our study. Although the exact mechanism for reduced platelet adsorption on the chitosan/CA fibers is unknown, we hypothesize that the hydrophilic chitosan coating in conjunction with the bound enzyme molecule may help prevent initial protein adsorption on the fiber surface, a known initiator of platelet adhesion and activation. Additionally, CA has been shown to naturally catalyze the formation of nitric oxide (NO) in blood [37], which is a potent inhibitor of platelet adhesion. Immobilized CA may act as a local catalytic source of NO, although further work is needed to confirm this hypothesis. Overall results indicate that the chitosan/CA coating may be a beneficial surface for preventing platelet adhesion, although SEM images indicate potential platelet degranulation which is a sign of platelet activation. Further work is necessary to quantify other hemocompatibility properties of the membrane coating, such as platelet activation, blood clotting times, and thrombus formation. Of note, SEM images of the chitosan and chitosan/CA fibers illustrate some surface heterogeneity in the coating, potentially due to chitosan/CA aggregates physically adsorbing to the fiber surface. However, we did not observe any coating stability deficiencies throughout this study, perhaps due to the insolubility of chitosan at physiologic pH. We are currently optimizing the immobilization chemistry to improve coating homogeneity.

Gas exchange modules using HFMs coated with chitosan and CA improved CO_2 removal rates 115 % in PBS buffer and 37 % in blood, compared to unmodified control HFMs. Reduced enhancement in blood can be interpreted as competition between immobilized CA on the fiber surface, and endogenous CA in circulating red blood cells within the device. In blood, endogenous CA helps maintain bulk phase pCO_2 by continually catalyzing HCO_3^- into gaseous CO_2, as CO_2 is removed by the device. This phenomenon helps improve overall CO_2 removal in blood compared to PBS buffer, but reduces the effect of immobilized CA. We are exploring methodologies to improve the impact of the CA coating on CO_2 removal enhancement in blood, through both biochemical modifications to the coating, and device design. For example, preliminary results incorporating a dilute acidic gas into the O_2 sweep gas stream demonstrated significantly enhanced CO_2 removal using chitosan/CA coated HFMs in blood, by forcing the $CO_2 + H_2O \overset{CA}{\rightleftharpoons} HCO_3^- + H^+$ chemical equilibrium towards CO_2 production by continual flux of H^+ into the bulk fluid (unpublished work). Further strategies to improve the performance of the chitosan/CA coating in blood will be important steps towards future use of the technology in clinical $ECCO_2R$ devices.

Certain aspects of this study are limited by the use of scaled down prototype gas exchange devices to characterize chitosan/CA coating effects on CO_2 removal. CO_2 mass transport

within the gas exchange device is governed by numerous coupled processes, including interconversion between HCO_3^- and CO_2 in the bulk fluid, diffusion of species through the blood-side liquid boundary layer, and CO_2 catalysis at the fiber surface by immobilized CA. Although CA has an extremely fast catalytic rate (1×10^6 s^{-1}), in the current prototype design, CO_2 transport is limited by boundary layer diffusion. However, active blood mixing devices which increase local blood velocities at the fiber surface and subsequently reduce boundary layer resistance may enhance the relative effect of immobilized CA on CO_2 removal. As such, coating immobilization chemistry must be validated on a device-specific basis. Furthermore, stability of the coating and glutaraldehyde crosslinking must be examined for extended use in blood (~7 days) to determine practical clinical utility of the coating technology. Lastly, hemocompatibility should be characterized under clinically relevant blood flows, to mimic appropriate shear forces and potential deleterious effects on platelets and red blood cells. Although the data presented here demonstrated positive platelet deposition results, further studies are necessary to characterize coating effects on device hemocompatibility.

5 Conclusions

$ECCO_2R$ is a promising therapeutic modality for the treatment of acute respiratory failure. Gas exchange membranes which facilitate high efficiency CO_2 removal may promote the development of smaller, ambulatory, and minimally invasive devices. The chitosan/CA fiber coating described in this work is a simple and effective coating for improving CO_2 removal efficiency while promoting favorable hemocompatibility properties of the membrane surface. Future work will focus on improving CO_2 removal efficacy in blood, further optimizing hemocompatibility characteristics of the bioactive membrane, and testing the chitosan/CA coating in an in vivo animal model.

Acknowledgments

Funding assistance for this work was provided by the National Institutes of Health: RO1HL70051 and T32HL07612403. The surface analysis experiments done at NESAC/BIO were supported by NIH Grant number EB-002027 from the National Institute of Biomedical Imaging and Bioengineering. The Postdoctoral Scholar appointment held by Dr. Jeremy Kimmel was supported by a Gift Award from ALung Technologies and the McGowan Institute for Regenerative Medicine. Recombinant human CA was kindly provided by Dr. David Silverman and Dr. Robert McKenna at the University of Florida.

References

1. Crotti S, Lissoni A, Tubiolo D, Azzari S, Tarsia P, Caspani L, et al. Artificial lung as an alternative to mechanical ventilation in COPD exacerbation. Eur Respir J. 2012; 39:212–5. [PubMed: 22210812]
2. Terragni PP, Del Sorbo L, Mascia L, Urbino R, Martin EL, Birocco A, et al. Tidal volume lower than 6 ml/kg enhances lung protection: role of extracorporeal carbon dioxide removal. Anesthesiology. 2009; 111:826–35. [PubMed: 19741487]
3. Alp E, Voss A. Ventilator associated pneumonia and infection control. Ann Clin Microbiol Antimicrob. 2006; 5:7. [PubMed: 16600048]
4. Ranieri VM, Suter PM, Tortorella C, De Tullio R, Dayer JM, Brienza A, et al. Effect of mechanical ventilation on inflammatory mediators in patients with acute respiratory distress syndrome: a randomized controlled trial. JAMA. 1999; 282:54–61. [PubMed: 10404912]
5. Alp E, Güven M, Yildiz O, Aygen B, Voss A, Doganay M. Incidence, risk factors and mortality of nosocomial pneumonia in intensive care units: a prospective study. Ann Clin Microbiol Antimicrob. 2004; 3:17. [PubMed: 15369593]
6. Chelluri L, Im KA, Belle SH, Schulz R, Rotondi AJ, Donahoe MP, et al. Long-term mortality and quality of life after prolonged mechanical ventilation. Crit Care Med. 2004; 32:61–9. [PubMed: 14707560]

7. Conrad S, Zwischenberger J, Grier L, Alpard S, Bidani A. Total extracorporeal arteriovenous carbon dioxide removal in acute respiratory failure: a phase I clinical study. Intensive Care Med. 2001; 27:1340–51. [PubMed: 11511947]
8. Pesenti A, Patroniti N, Fumagalli R. Carbon dioxide dialysis will save the lung. Crit Care Med. 2010; 38:S549–54. [PubMed: 21164396]
9. Terragni P, Maiolo G, Ranieri VM. Role and potentials of low-flow CO(2) removal system in mechanical ventilation. Curr Opin Crit Care. 2012; 18:93–8. [PubMed: 22186219]
10. Stirling SL, Cordingley JJ, Hunter DN, Griffiths MJ, Wort SJ, Evans TW, et al. Extracorporeal carbon dioxide removal to “protect” the Lung. Thorax. 2009; 64:726–7. [PubMed: 19638565]
11. Ruberto F, Pugliese F, D’Alio A, Perrella S, D’Auria B, Ianni S, et al. Extracorporeal removal CO_2 using a venovenous, low-flow system (Decapsmart) in a lung transplanted patient: a case report. Transpl Proc. 2009; 41:1412–4.
12. Arazawa DT, Oh H-I, Ye S-H, Johnson CA Jr, Woolley JR, Wagner WR, et al. Immobilized carbonic anhydrase on hollow fiber membranes accelerates CO_2 removal from blood. J Membr Sci. 2012; 403–404:25–31.
13. Kaar JL, Oh H-I, Russell AJ, Federspiel WJ. Towards improved artificial lungs through biocatalysis. Biomaterials. 2007; 28:3131–9. [PubMed: 17433433]
14. Batchinsky AI, Jordan BS, Regn D, Necsoiu C, Federspiel WJ, Morris MJ, et al. Respiratory dialysis: reduction in dependence on mechanical ventilation by venovenous extracorporeal CO_2 removal. Crit Care Med. 2011; 39:1382–7. [PubMed: 21317644]
15. Wearden P, Federspiel W, Morley S, Rosenberg M, Bieniek P, Lund L, et al. Respiratory dialysis with an active-mixing extra-corporeal carbon dioxide removal system in a chronic sheep study. Intensive Care Med. 2012; 38(10):1705–11. [PubMed: 22926651]
16. Manta C, Ferraz N, Betancor L, Antunes G, Batista-Viera F, Carlsson J, et al. Polyethylene glycol as a spacer for solid-phase enzyme immobilization. Enzyme Microb Technol. 2003; 33:890–8.
17. Wan J, Thomas MS, Guthrie S, Vullev VI. Surface-bound proteins with preserved functionality. Ann Biomed Eng. 2009; 37:1190–205. [PubMed: 19308733]
18. Wang Y, Hsieh Y-L. Enzyme immobilization to ultra-fine cellulose fibers via amphiphilic polyethylene glycol spacers. J Polym Sci Part Polym Chem. 2004; 42:4289–99.
19. Goddard JM, Hotchkiss JH. Polymer surface modification for the attachment of bioactive compounds. Prog Polym Sci. 2007; 32:698–725.
20. Goddard JM, Talbert JN, Hotchkiss JH. Covalent attachment of lactase to low-density polyethylene films. J Food Sci. 2007; 72:E036–41. [PubMed: 17995883]
21. Kingshott P, Wei J, Bagge-Ravn D, Gadegaard N, Gram L. Covalent attachment of poly(ethylene glycol) to surfaces, critical for reducing bacterial adhesion. Langmuir. 2003; 19:6912–21.
22. Aranaz I, Mengibar M, Harris R, Panos I, Miralles B, Acosta N, et al. Functional characterization of chitin and Chitosan. Curr Chem Biol. 2009; 3:203–30.
23. Zhang Y, Li L, Yu C, Hei T. Chitosan-coated polystyrene microplate for covalent immobilization of enzyme. Anal Bioanal Chem. 2011; 401(7):2311–7. [PubMed: 21842444]
24. Delanoy G, Li Q, Yu J. Activity and stability of laccase in conjugation with chitosan. Int J Biol Macromol. 2005; 35:89–95. [PubMed: 15769520]
25. Hung T-C, Giridhar R, Chiou S-H, Wu W-T. Binary immobilization of Candida rugosa lipase on chitosan. J Mol Catal B Enzym. 2003; 26:69–78.
26. Fisher SZ, Tu C, Bhatt D, Govindasamy L, Agbandje-McKenna M, McKenna R, et al. Speeding up proton transfer in a fast enzyme: kinetic and crystallographic studies on the effect of hydrophobic amino acid substitutions in the active site of human carbonic anhydrase II. Biochemistry (Mosc). 2007; 46:3803–13.
27. Cook AD, Pajvani UB, Hrkach JS, Cannizzaro SM, Langer R. Colorimetric analysis of surface reactive amino groups on poly (lactic acid-co-lysine): poly (lactic acid) blends. Biomaterials. 1997; 18:1417–24. [PubMed: 9375843]
28. Eash HJ, Jones HM, Hattler BG, Federspiel WJ. Evaluation of plasma resistant hollow fiber membranes for artificial lungs. ASAIO. 2004; 50:491–7.

29. Federspiel WJ, Hattler BG. Sweep gas flowrate and CO_2 exchange in artificial lungs. Artif Organs. 1996; 20:1050–2. [PubMed: 8864027]
30. Tamada Y, Kulik EA, Ikada Y. Simple method for platelet counting. Biomaterials. 1995; 16:259–61. [PubMed: 7749004]
31. Lund LW, Hattler BG, Federspiel WJ. Gas permeance measurement of hollow fiber membranes in gas-liquid environment. AI-ChE J. 2002; 48:635–43.
32. Kayastha AM, Srivastava PK. Pigeonpea (*Cajanus cajan* L.) urease immobilized on glutaraldehyde-activated chitosan beads and its analytical applications. Appl Biochem Biotechnol. 2001; 96:041–54.
33. Rodrigues DS, Mendes AA, Adriano WS, Gonçalves LRB, Giordano RLC. Multipoint covalent immobilization of microbial lipase on chitosan and agarose activated by different methods. J Mol Catal B Enzym. 2008; 51:100–9.
34. Tyan Y-C, Liao J-D, Lin S-P. Surface properties and in vitro analyses of immobilized chitosan onto polypropylene non-woven fabric surface using antenna-coupling microwave plasma. J Mater Sci Mater Med. 2003; 14:775–81. [PubMed: 15348397]
35. Liao J-D, Lin S-P, Wu Y-T. Dual properties of the deacetylated sites in chitosan for molecular immobilization and biofunctional effects. Biomacromolecules. 2005; 6:392–9. [PubMed: 15638544]
36. Rao SB, Sharma CP. Use of chitosan as a biomaterial: studies on its safety and hemostatic potential. J Biomed Mater Res. 1997; 34:21–8. [PubMed: 8978649]
37. Aamand R, Dalsgaard T, Jensen FB, Simonsen U, Roepstorff A, Fago A. Generation of nitric oxide from nitrite by carbonic anhydrase: a possible link between metabolic activity and vasodilation. Am J Physiol Heart Circ Physiol. 2009; 297:H2068–74. [PubMed: 19820197]

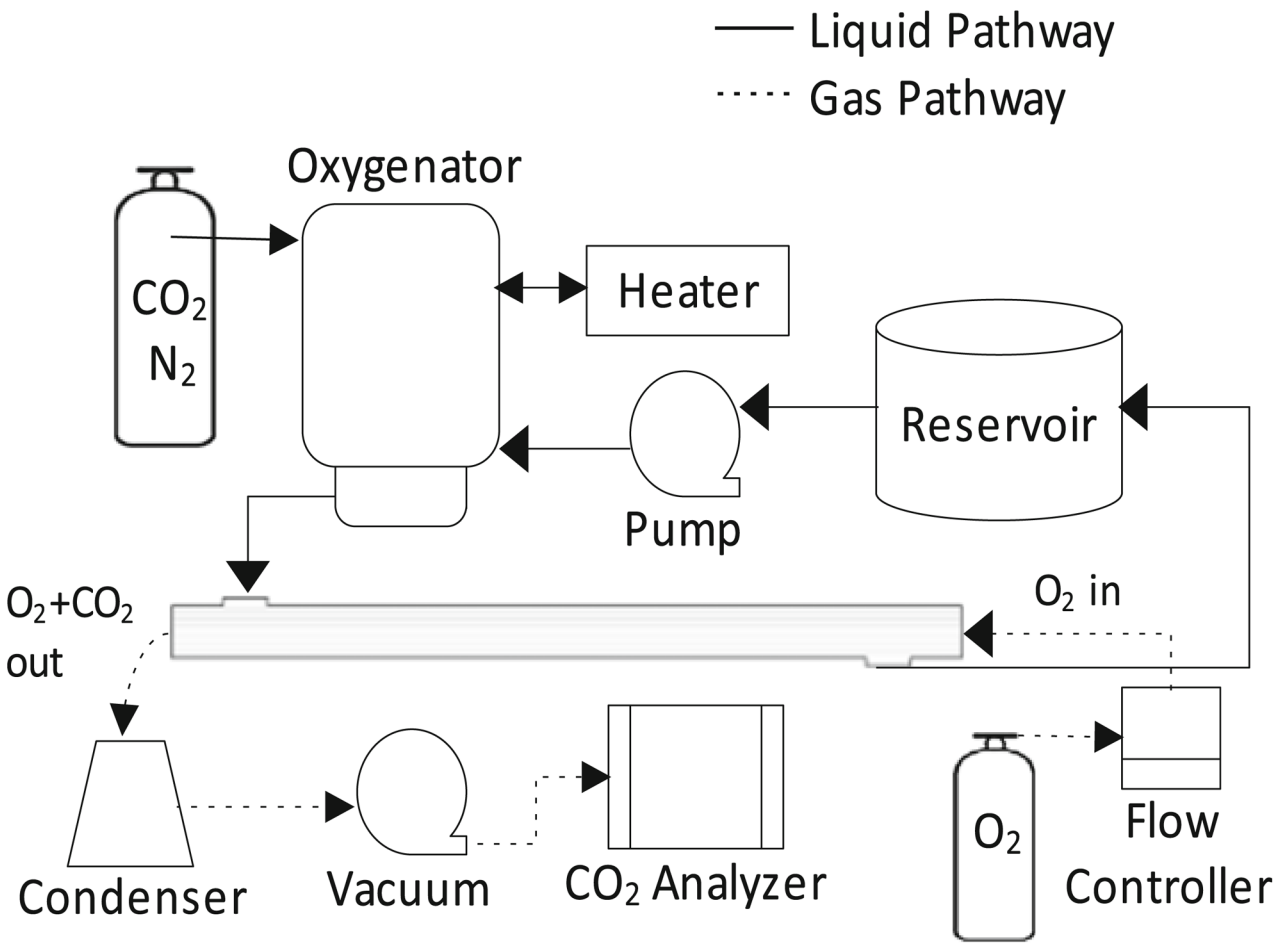

Fig. 1.
Schematic of the in vitro gas exchange test loop

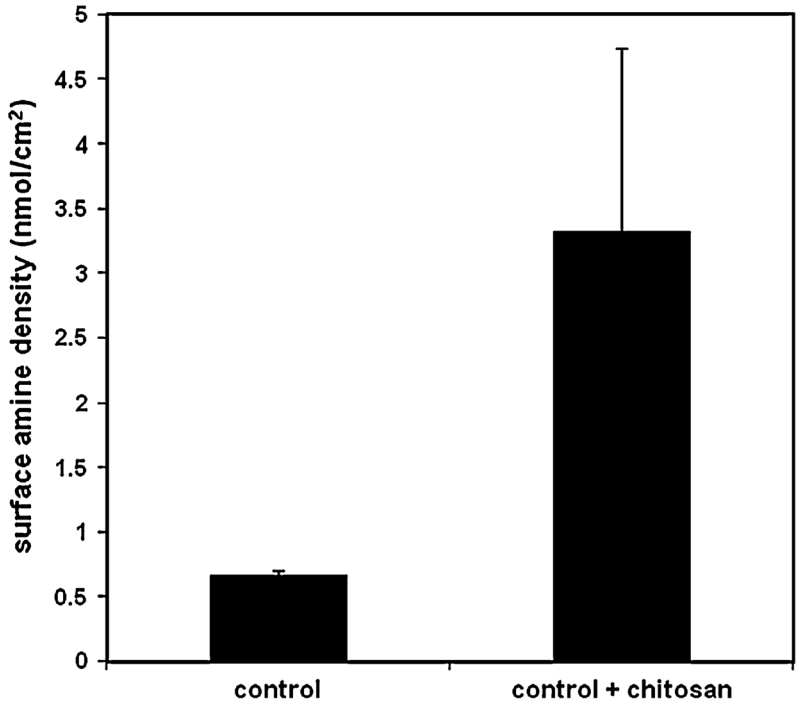

Fig. 2.
Fiber surface amine density, quantified using a colorimetric sulfo-SDTB assay

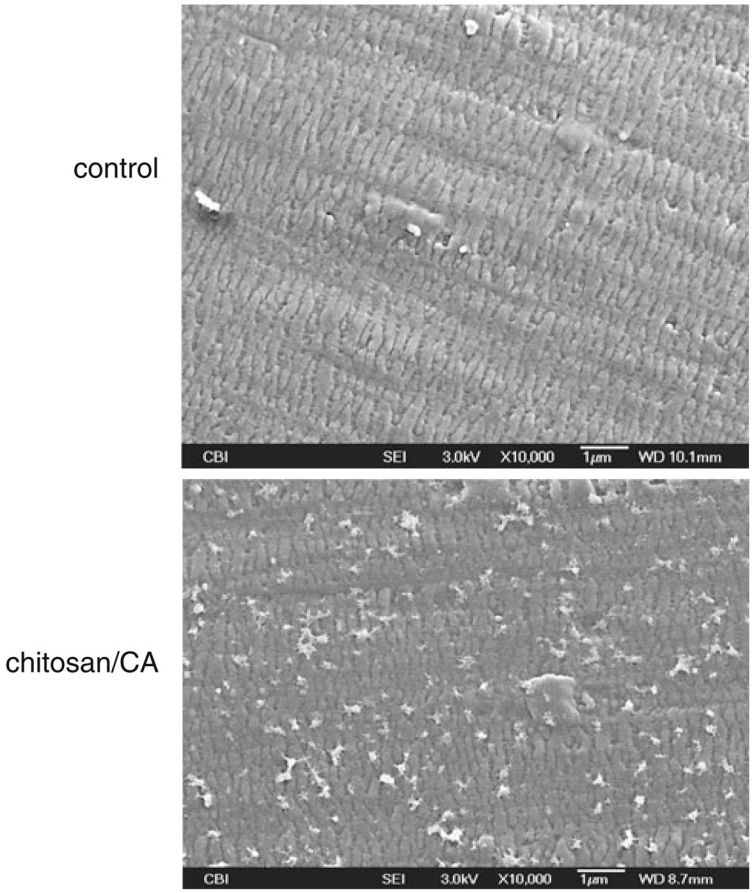

Fig. 3.
SEM surface images of unmodified control fiber, and fiber after chitosan+CA immobilization

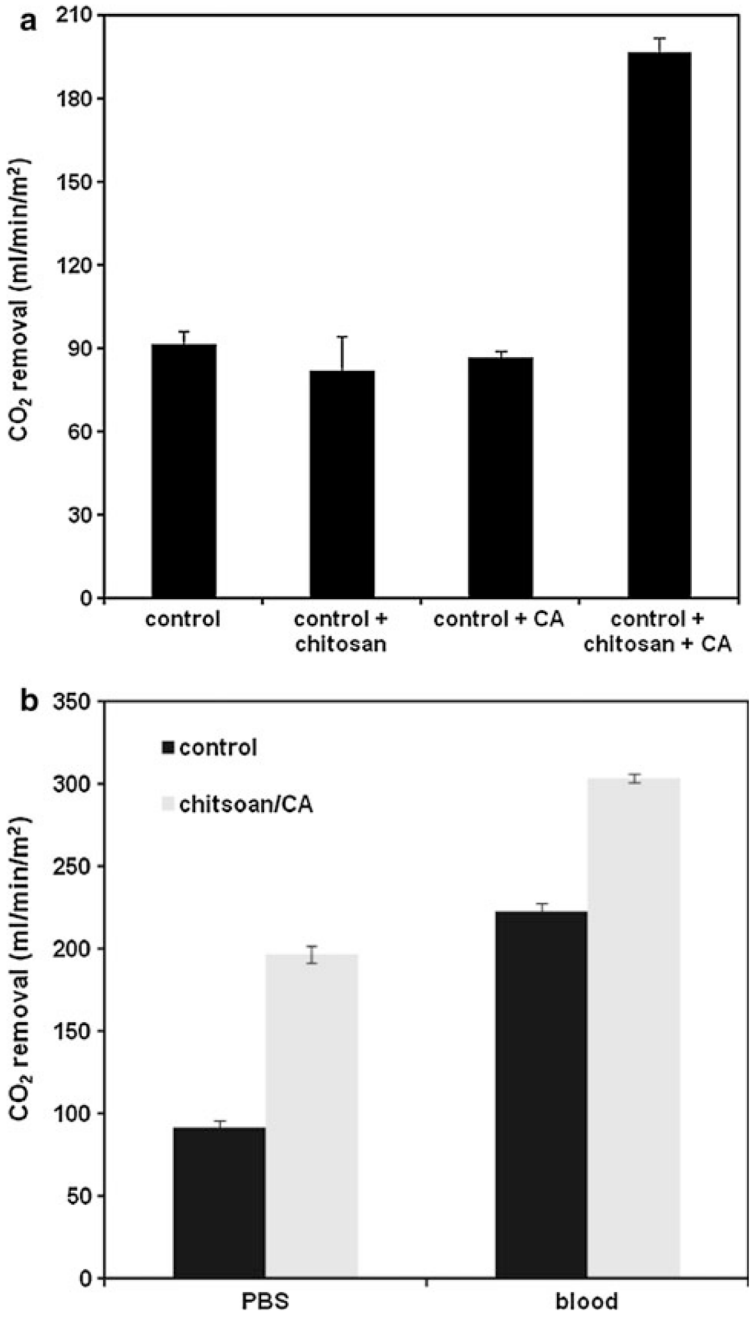

Fig. 4.

a CO_2 removal rates in PBS for gas exchange modules modified with chitosan, CA, or chitosan+CA. Control fibers are siloxane/aminated without further modification. **b** CO_2 removal rates for gas exchange modules in PBS and bovine blood. Chitsoan/CA modules demonstrate 115 % enhancement compared to unmodified control modules in PBS, and 37 % enhancement in blood

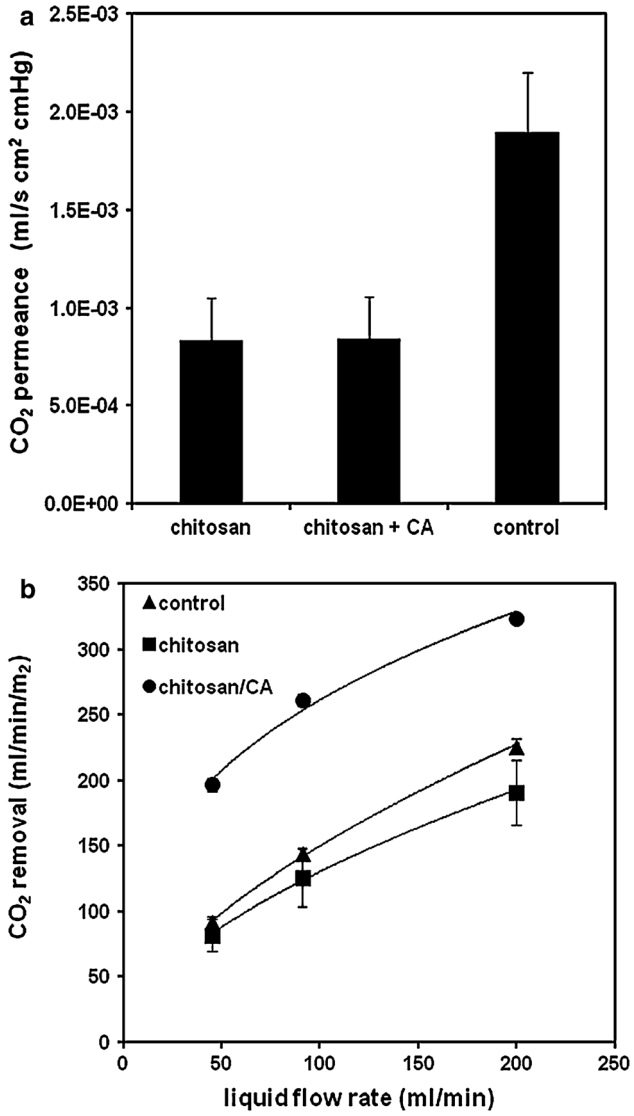

Fig. 5.

a CO_2 gas permeance of chitosan, chitosan+CA, and control fibers. **b** CO_2 removal rates in PBS under varying liquid flow rates through the gas exchange module

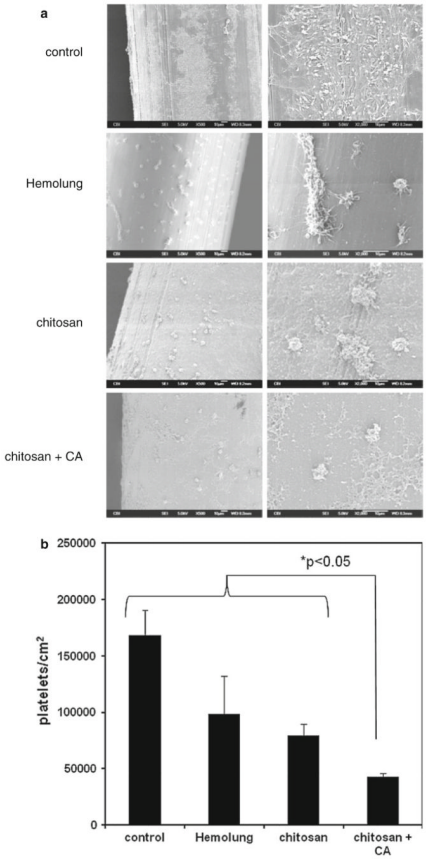

Fig. 6.

a Scanning electron micrographs of fiber surfaces after contact with heparinized ovine blood for 2 h at 37 °C. **b** Platelet deposition on HFM surfaces after contact with heparinized ovine blood quantified by a lactate dehydrogenase (LDH) assay

Table 1

XPS atomic surface composition for control fiber and chitosan immobilized fibers

	C1s	O1s	Si2p	N1s
Control	41.0 ± 2.2	33.6 ± 0.3	23.8 ± 2.1	1.6 ± 0.2
Chitosan	54.2 ± 0.9	29.3 ± 0.6	12.9 ± 0.6	3.6 ± 0.5